RSC Advances

PAPER

View Article Online
View Journal | View Issue

Cite this: *RSC Adv.*, 2026, **16**, 11061

Exploration of the aromatic abietane diterpenoid scaffold in the development of ArnT-mediated colistin resistance inhibitors

Silvia Cammarone, †[a] Valentina Pastore,†[b] Mariya Ryzhuk,[a] Martina Cristoferi,[b] Arianna Speroni,[a] Francesco Imperi,[c] Davide Corinti,[a] Maria Carmela Bonaccorsi di Patti,[d] Bruno Botta,[a] Deborah Quaglio,*[a] Mattia Mori,*[e] Fiorentina Ascenzioni[b] and Francesca Ghirga[a]

Colistin is a last-resort antibiotic for treating multidrug-resistant Gram-negative bacterial infections. However, some bacteria, such as *Pseudomonas aeruginosa*, can develop resistance to colistin thanks to the modification of the lipid A component of the outer membrane catalyzed by the 4-amino-4-deoxy-L-arabinose transferase ArnT. Here, building on our previous identification of the natural *ent*-beyerene diterpene **FDO** as an ArnT inhibitor, we report a rational procedure to simplify the *ent*-beyerene scaffold into drug-like synthetic ArnT inhibitors. Starting from the aromatic abietane scaffold of podocarpic acid **1**, a function-oriented synthesis (FOS) approach guided the preparation of twenty-four semisynthetic oxygen and nitrogen abietane-based derivatives. Biological evaluation against a colistin-resistant *P. aeruginosa* strain revealed that four compounds (**2**, **13**, **18**, and **30**) significantly restore the activity of sub-inhibitory colistin, with compound **18** showing the lowest IC_{90} (182.5 μM). Structure–activity relationship (SAR) studies revealed that positions C-12 and C-16 are critical for activity, while molecular docking suggested that the selected analogs can engage in interactions with conserved residues within the ArnT catalytic site. Microbiological assays highlighted key structural features of the aromatic abietane skeleton in restoring colistin sensitivity in drug-resistant *P. aeruginosa*, and rationalized biological activity data to corroborate the quality of the selected scaffold in the development of cost-effective colistin resistance breakers.

Received 26th November 2025
Accepted 5th February 2026

DOI: 10.1039/d5ra09142j

rsc.li/rsc-advances

Introduction

Global resistance to most available antibiotics is threatening human health and making antibiotic choices for infection control limited and more expensive.[1] In particular, the emergence of multidrug-resistant (MDR) pathogens such as *Pseudomonas aeruginosa*, *Acinetobacter baumannii*, and Enterobacteriaceae is alarming.[2] Hence, in 2017, the World Health Organization (WHO) included these pathogens in the list of bacteria for which antibiotics are urgently needed as a priority.[3]

Although new treatment options such as ceftazidime/avibactam, ceftolozane/tazobactam (Avycaz®), (Zerbaxa®), plazomicin (Zemdri®), and eravacycline (Xerava®) have become available for the treatment of Gram-negative bacteria, resistance to these treatments has already started to emerge.[4] Thus, the medical community re-evaluated the use of old antibiotics, such as polymyxins, including colistin and polymyxin B.[5–7] The reintroduction of colistin in clinical practice has inevitably led to the emergence and spread of colistin-resistant isolates, as evidenced by numerous case reports.[8] Colistin targets the lipopolysaccharide (LPS) of the outer membrane (OM) of Gram-negative bacteria by electrostatic interaction, which in turn displaces the OM stabilizing cations, Mg^{2+} and Ca^{2+}, causing OM destabilization, leakage of cell contents, and ultimately cell death. More recently, it has been proposed that colistin binding to newly synthesized LPS in the cytoplasmic membrane (CM) also contributes to its bactericidal activity.[9] Accordingly, accumulation of LPS in the CM increases the susceptibility of *P. aeruginosa* to colistin.[9] Therefore, to counteract the antimicrobial activity of colistin, bacteria have developed mechanisms to decrease the overall charge of LPS, which in turn reduces the binding affinity of the cationic lipopeptide and its bactericidal

[a]*Department of Chemistry and Technology of Drugs, Sapienza University of Rome, Italy. E-mail: deborah.quaglio@uniroma1.it*

[b]*Department of Biology and Biotechnology Charles Darwin, Sapienza University of Rome, Italy*

[c]*Department of Science, Roma Tre University, Italy*

[d]*Department of Biochemical Sciences "A. Rossi Fanelli" Sapienza University of Rome, Italy*

[e]*Department of Biotechnology, Chemistry and Pharmacy, University of Siena, Italy. E-mail: mattia.mori@unisi.it*

† These authors contributed equally to this work.

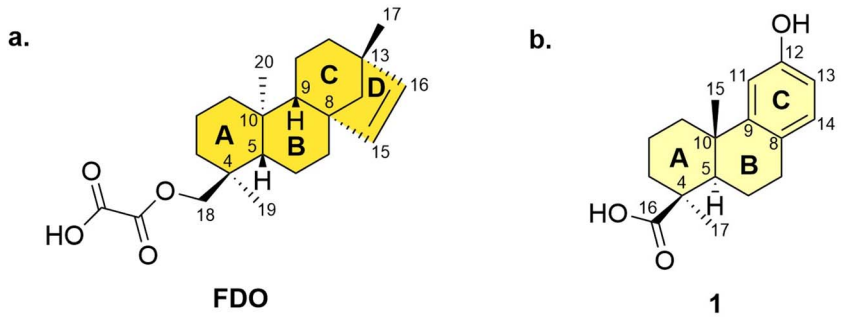

Fig. 1 Chemical structures of the ent-beyerene diterpene FDO (a) and aromatic abietane podocarpic acid (1) (b).

activity.[7] Although different mechanisms of LPS modification have been described, including the addition of phosphoethanoamine (pEtN) or 4-amino-4-deoxy-L-arabinose (L-Ara4N) to the lipid A component of LPS,[10–12] in *P. aeruginosa* the latter is the major colistin resistance mechanism.[10,13] This mechanism, which is activated by mutations in two-component regulatory systems, such as PmrAB and PhoPQ, is mediated by the *arn* operon, and requires multiple steps, the final one being the transfer of L-Ara4N to lipid A by the integral CM enzyme ArnT (undecaprenyl phosphate-alpha-4-amino-4-deoxy-L-arabinose arabinosyl transferase).[7] ArnT catalyzes the transfer of L-Ara4N, provided by the lipid carrier undecaprenyl phosphate, to lipid A phosphate groups.[14]

Enhancing the effectiveness of existing antimicrobial compounds is a promising strategy for addressing the current antibiotic resistance crisis. Specifically, inhibitors of key enzymes involved in antibiotic resistance offer an alternative approach to combating this threat. Remarkably, only a few examples of colistin adjuvants have been reported to date.[15,16] By combining these inhibitors with clinically relevant antibiotics, we can potentially prolong the lifespan of these antibacterial drugs and reduce the impact of resistance. Notwithstanding, identifying novel classes of these life-saving drugs has become more challenging, requiring new paradigms. In the current scenario, exploring the biologically relevant chemical space of natural products (NPs) remains a promising approach for discovering novel antimicrobial or antibiotic adjuvants.[17–22] Indeed, several design strategies were employed to develop novel and fascinating architectures by skillfully manipulating the NP's core scaffold.[20,21,23]

In a previous work, we have identified the *ent*-beyerene diterpene **FDO** (formerly known as BBN149), isolated from the leaves of *Fabiana densa* var. *ramulosa*, a native shrub of Chile, as a potent ArnT inhibitor capable of restoring colistin efficacy in resistant *P. aeruginosa* strains without significantly affecting colistin-susceptible strains (Fig. 1a).[24–27] These results suggest that **FDO** prevents lipid A aminoarabinosylation, likely by inhibiting ArnT enzymatic activity, thus restoring colistin efficacy.[25] A large variety of chemical analogs was produced for SAR studies to validate the potential of the diterpene scaffold as a key platform for the further development of ArnT-mediated colistin resistance inhibitors with improved activity.[27] However, notable challenges are associated with this type of diterpene, including the low concentration of the compound in the Chilean plant *F. densa* var. *ramulosa*, the need for multistep purification of the raw material, the absence of chromophore groups and low solubility. The latter was recently addressed by the development of liposomal carriers for the co-delivery of colistin and diterpenoid ArnT inhibitors.[28]

Here, to address these issues, we considered rational procedures that simplify the *ent*-beyerene complex structure into drug-like synthetic molecules, thereby minimizing the pharmacophore structures that are crucial for biological activity. Therefore, other naturally related diterpene scaffolds were evaluated as starting materials to prepare a novel generation of ArnT inhibitors. In particular, we investigated the aromatic abietane scaffold, which lacks ring D compared to the *ent*-beyerene one and features an aromatic ring C and varying degrees of oxygenation at several positions.[29] Several synthetic studies that aim to modify the abietane skeleton to obtain novel biologically active compounds have been reported. To achieve this, naturally occurring terpenoids, which are available in large quantities, were utilized as enantiomerically pure starting materials for the synthesis of bioactive abietanes.[30] In this study, we report the design, synthesis, and biological evaluation of a series of novel abietane-based derivatives derived from podocarpic acid **1** (Fig. 1b), conceived as function-oriented analogs of the natural *ent*-beyerene hit **FDO** (Fig. 1a).

By exploiting the structural modularity of the abietane scaffold and guided by *in silico* modeling, we aimed to identify simplified and synthetically accessible compounds capable of selectively inhibiting ArnT and restoring colistin efficacy against resistant *P. aeruginosa* strains. This work highlights the potential of aromatic diterpenoids as a viable chemical platform and FOS as a successful design strategy for the development of next-generation colistin resistance inhibitors.

Results and discussion

Rational design strategy

Recently, we demonstrated that an *ent*-beyerene scaffold bearing an oxalate-like group at C-18/C-19 or a sugar residue at C-19 is an essential requirement for efficient inhibition of bacterial growth in the presence of colistin, likely resulting from a more efficient inhibition of the ArnT activity.[27] Here, we simplified the complex structure of *ent*-beyerene through a function-oriented synthesis (FOS) approach to optimize the hit compound by minimizing the crucial pharmacophores

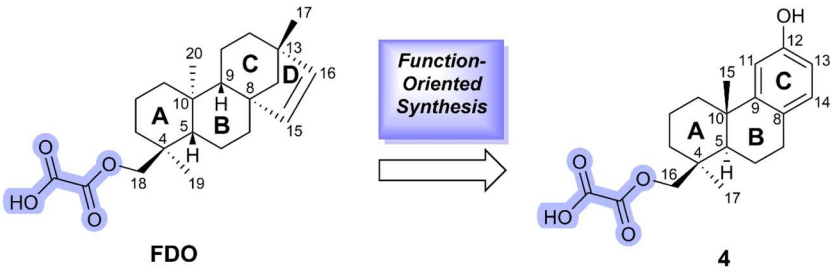

Fig. 2 The *hit* compound FDO and the simplified aromatic analog **4**. The key binding element is highlighted in blue.

necessary for biological activity.[31,32] In particular, this study investigates the aromatic abietane scaffold of **1**, which lacks the ring D compared to the *ent*-beyerene one, maintains the same configuration at C-4 concerning **FDO**, and features an aromatic ring C and a hydroxyl group at the C-12 position. Based on a function-oriented design, compound **4**, in which the abietane scaffold of **1** incorporates the key recognition feature of the hit **FDO**, the oxalyl group at C-16, was designed (Fig. 2) and evaluated *in silico* towards the predicted structure of *P. aeruginosa* ArnT by adapting from the computational protocol already established and validated in previous works.[25,27]

The abietane scaffold of **1** was prioritized for further experimental investigations due to its potential interaction with the target receptor as well as functionalization strategies. We synthesized a focused library of twenty-four derivatives of **1**, combining the aromatic abietane scaffold with key binding elements essential for efficient inhibition of ArnT activity, as previously investigated in SAR studies of the *ent*-beyerene derivatives.[27] In particular, different derivatives of **1** were synthesized to investigate the role of (i) the oxalyl group at C-16, an essential requirement for the ArnT activity inhibition of the hit compound **FDO**; (ii) the length and flexibility of the alkyl chain of the functional group at C-16; (iii) the presence of a sugar unit to mimic L-Ara4N; (iv) the substitution of the oxygen with nitrogen heteroatom in the functional group at C-16 on the biological properties of the original abietane scaffold; and (v) the role of the phenolic group at C-12.

Chemistry

Commercially available **1** was used as the starting material for preparing derivatives of the oxygen series (**2–8**, **12–18**) and the nitrogen series (**19–26**, **30–31**).

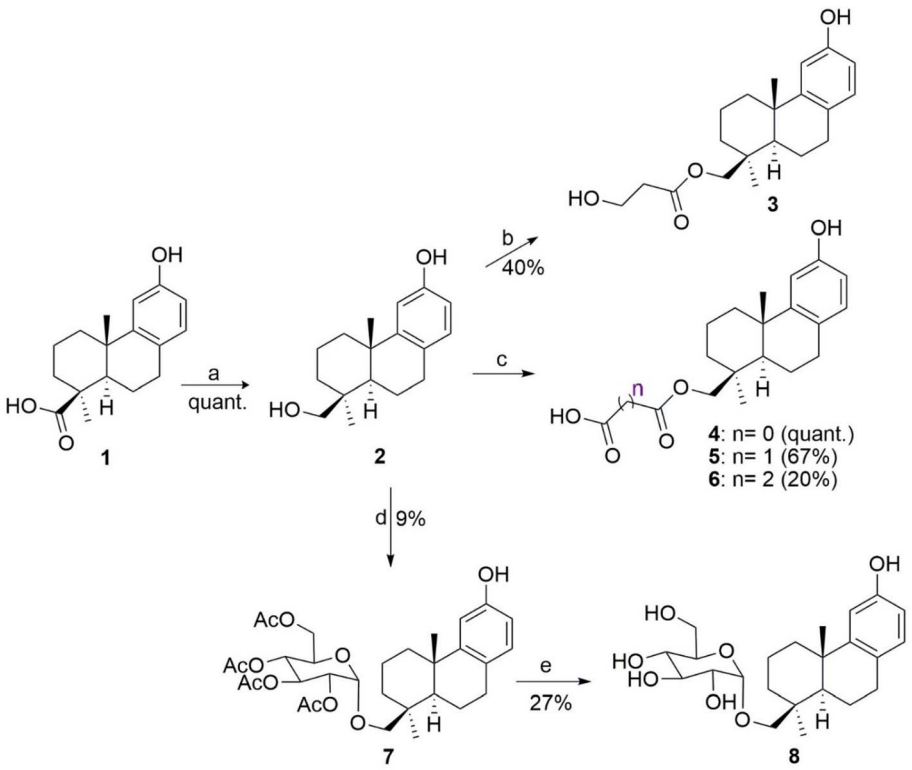

Scheme 1 Reagents and conditions. (a) (1) $SOCl_2$, 76 °C, 4 h; (2) $LiAlH_4$, dry THF, r.t., 24 h; (b) $COOH(CH_2)_2OTBS$, $SOCl_2$, CH_2Cl_2/THF, 50 °C to r.t., o/n; (c) $ClCO(CH_2)_nCOCl$, Et_2O, 0 °C to r.t., 30 min.; (d) acetobromo-a-D-glucose, $ZnCl_2$, CH_2Cl_2, 50 °C, 24 h; (e) MeOH/Et_3N/H_2O, r.t., 36 h.

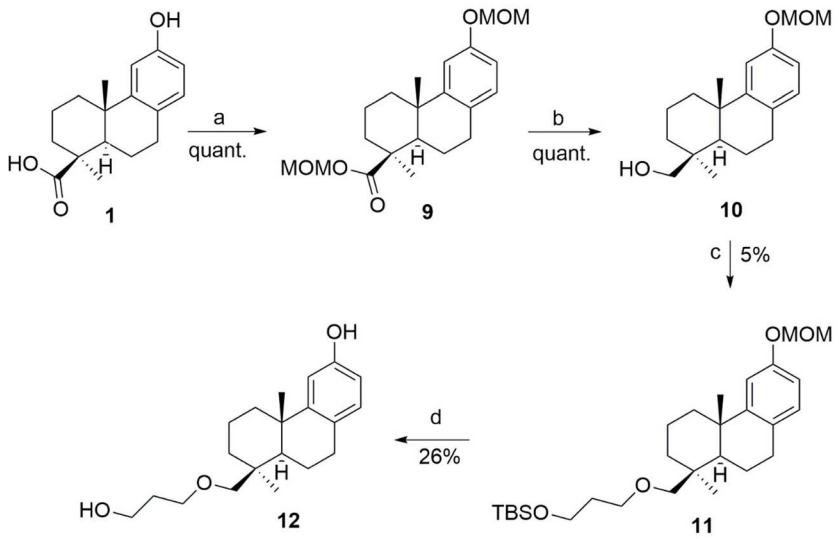

Scheme 2 Reagents and conditions. (a) MOMCl, DIPEA, dry CH_2Cl_2, r.t., 48 h; (b) $LiAlH_4$ 2 M in THF, dry THF, 0 °C to r.t., 2.5 h; (c) **BrP-TBS***, NaH, DMF, r.t., 24h; (d) TFA, TFE, CH_2Cl_2, 0 °C to r.t., 5 h. *for preparation of **BrP-TBS** see SI (Scheme S1).

Oxygen (O) series

According to the SAR analysis previously performed on the *ent*-beyerene scaffold, we designed and synthesized a small focus library of **1** *O*-derivatives bearing an alcohol or an oxalate-like group or a sugar residue at C-16 (**2–8**) (Scheme 1).

To specifically assess whether the removal of the carbonyl groups at C-16 could affect the colistin adjuvant activity, alcohol **2** was prepared in quantitative yield through a synthetic approach that involved a first activation of carboxylic acid to the corresponding acyl chloride, followed by the reduction of the carbonyl group of **1** using lithium aluminum hydride ($LiAlH_4$). This compound was then used to synthesize derivatives **3–8** by chemical modifications of the alcohol group at C-16. In particular, to investigate the role of the distance between the lipophilic portion of the terpene scaffold and the polar function, the alcohol group linked at position C-16, compound **3** was obtained in 40% yield *via* condensation reaction of **2** with commercially available 3-[(*tert*-butyldimethylsilyl)oxy]propanoic acid previously activated to acyl chloride (Scheme S1). Indeed, to evaluate the length and flexibility of the alkyl chain of the functional group at C-16, the corresponding oxalyl **4**, malonyl **5**, and succinyl **6** esters were obtained by treating diterpene **2** with the corresponding acyl chloride in Et_2O at room temperature for 30 min, in quantitative, 67%, and 20% yields, respectively. Furthermore, to assess the influence of a sugar unit to mimic L-Ara4 N at C-16 position, the glycosidic derivative **7** was prepared by adding the alcohol **2** to a solution of acetobromo α-D-glucose and zinc chloride, according to the Koenigs–Knorr reaction.[33] Most commonly, the glycosylation reaction follows an unimolecular S_N1 mechanism, forming the resonance-stabilized oxocarbenium ion. As a result, the nucleophilic attack could occur almost equally from either the top (to give the 1,2-trans isomer or β) or the bottom face (to give the 1,2-cis or α isomer) of the ring. However, the anomeric effect promotes the α-glycosylation.[34] In particular, the formation of the alpha isomer was confirmed by ^{1}H-NMR analysis observing a coupling constant (*J*) of 3.36 Hz for the douplet signal centered at 5.03 ppm, related to the proton H1′ (the one on anomeric carbon). This value is characteristic of an eq-ax coupling, as typically observed between the protons H1′ and H2′.[35] Additionally, deacetylation of sugar hydroxyl groups *via* alkaline hydrolysis with triethylamine produced **8** in 27% yield. Lastly, to evaluate the effect of introducing a more flexible alkyl chain that enhances the distance between the lipophilic portion and the polar function of the abietane scaffold, alcohol **10** was prepared by first protecting **1** with chloromethyl methyl ether (MOMCl), followed by reduction using $LiAlH_4$ to obtain it in a quantitative yield (Scheme 2).

Protecting the phenolic group at position 12 as a methoxymethyl ether was necessary to prevent its etherification during the subsequent nucleophilic substitution reaction. Intermediate **10**, formed after the reduction with $LiAlH_4$, was then deprotonated with sodium hydride (NaH) to allow nucleophilic substitution with 3-bromo-1-propanol previously protected with tert-butyldimethylsilyl (TBS) (Scheme S1). Finally, a double deprotection of MOM and TBS was performed using trifluoroacetic acid (TFA) and trifluoroethanol (TFE) (1 : 1 ratio) in dichloromethane (DCM), resulting in the desired derivative **12** in 26% yield.

According to the docking study, an additional binding interaction at the aromatic C ring of the abietane scaffold of **1** may provide advantages in binding affinity compared to the reference molecule **FDO**. Therefore, to investigate the role of the phenolic group at C-12, the dimethylated ester **13** was prepared by treating **1** with methyl iodide (CH_3I) and potassium carbonate (K_2CO_3) as base, resulting in a 70% yield. The methyl ester **14** was also obtained in 30% yield. Compound **13** was further used for synthesizing derivatives **15–16**. In particular, hydrolysis of **13** led to the formation of acid **15** with an 80% yield. Compound **16** was prepared by reducing **13** with $LiAlH_4$ to the corresponding alcohol in a quantitative yield. Then, the

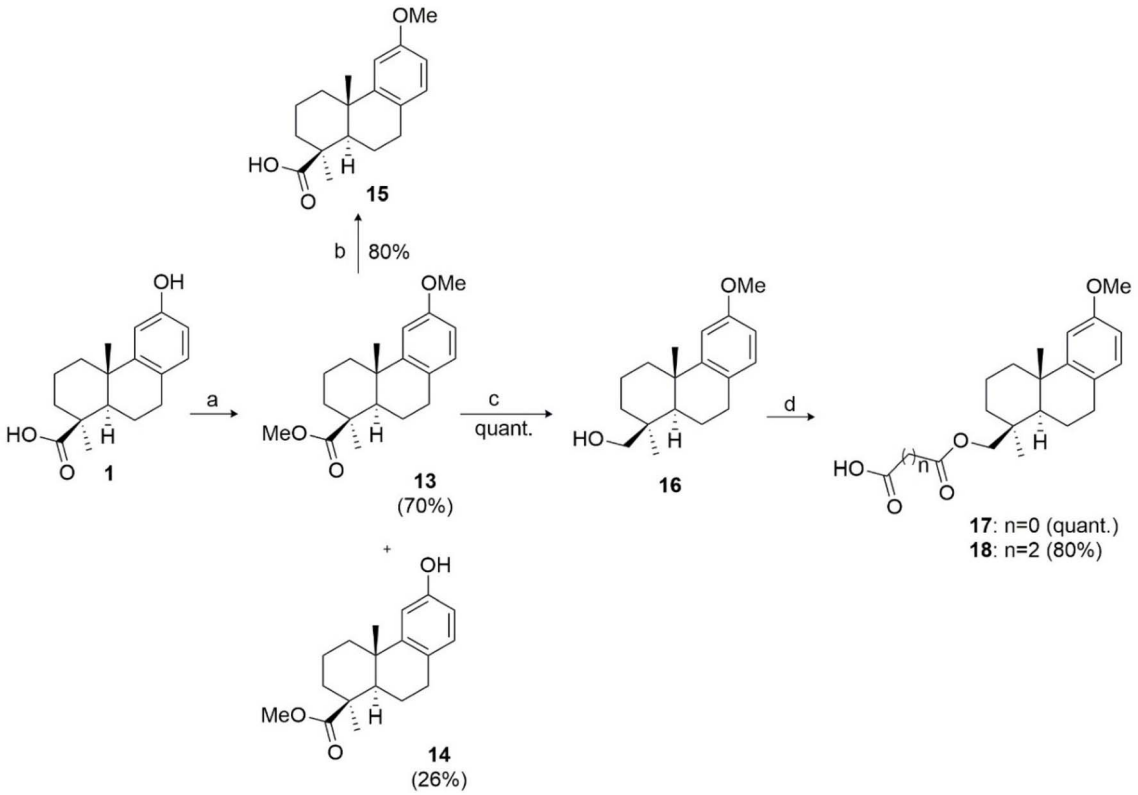

Scheme 3 Reagents and conditions. (a) CH_3I, K_2CO_3, acetone, 56 °C, 24 h; (b) *t*-BuOK, DMSO, 100 °C, 72 h; (c) $LiAlH_4$, dry THF, 0 °C to r.t. 24 h; (d) $ClCO(CH_2)_nCOCl$, Et_2O, 0 °C to r.t., 30 min.

hydroxyl group of **13** was esterified with the desired acyl chloride, resulting in the oxalyl ester **17** in quantitative yield and the succinyl ester **18** in 80% yield (Scheme 3).

Thus, derivatives **13**, **15**, **16**, **17** and **18** differ from the structurally correlated ones **14**, **1**, **2**, **4** and **6**, respectively, only due to the methoxyl group at C-12.

Nitrogen (N) series

A series of N-derivatives of compound **1**, featuring a primary or secondary amide or amine at the C-16 position, was designed according to bioisosterism. The aim was to assess whether replacing the oxygen atom with a nitrogen atom could affect the chemical stability and the effectiveness of inhibition of ArnT. Indeed, this chemical modification could facilitate compound entry and its accumulation according to the "eNTRy rules".[36] Accordingly, an efficient strategy for the preparation of the primary amide **19** was developed, involving the use of *N*,*N*-diisopropylethylamine (DIPEA), hexafluorophosphate azabenzotriazole tetramethyl uranium (HATU) as a coupling agent, and ammonium chloride (NH_4Cl).[37] This strategy, reported in the literature for amidation reactions, enabled the production of **19** in a single step with quantitative yield (Scheme 4).

Furthermore, reducing the carbonyl group of **19** using $LiAlH_4$ resulted in the corresponding primary amine **20** in 50% yield. Compound **21**, featuring an oxalate-like group at C-16, an essential requirement for the ArnT activity inhibition of the hit compound **FDO**, was obtained by amidation reaction of **20** with succinic anhydride and 4-dimethylaminopyridine (DMAP) as base in quantitative yield. This derivative differs from the structurally correlated one, **6**, only due to the substitution of the oxygen with a nitrogen atom at C-16. According to docking analysis, the introduction of an alkyl chain to enhance the distance between the lipophilic portion and the polar function (alcohol group) of the abietane scaffold was also investigated in this series. In particular, the secondary amide **22** was prepared using the same amidation reaction employed for **19**, by coupling **1** with β-alanine in the presence of HATU and DIPEA (Scheme 5).

Similarly, secondary amides **23–25** were synthesized by coupling **1** with the suitable linear amino alcohol in the presence of HATU and DIPEA, resulting in the corresponding *N*-hydroxypropyl, butyl, and pentyl amides **23–25** in 90%, quantitative and 85% yields, respectively (Scheme 5). Furthermore, amide **23** was reduced with $LiAlH_4$ to the corresponding secondary amine **26** in low yield (12% yield), whereas amides **24** and **25** showed no reactivity under the same reduction conditions. For this reason, a different procedure *via* reductive amination became necessary to obtain amines **30** and **31** (Scheme 6).

In particular, oxidation under mild conditions using Dess–Martin Periodinane (DMP) as the oxidizing agent of alcohol **11**, previously obtained as shown in Scheme 2, led to the aldehyde **27** in 65% yield.[38] This intermediate underwent a reductive amidation reaction with the suitable amino-alcohol,[39] followed

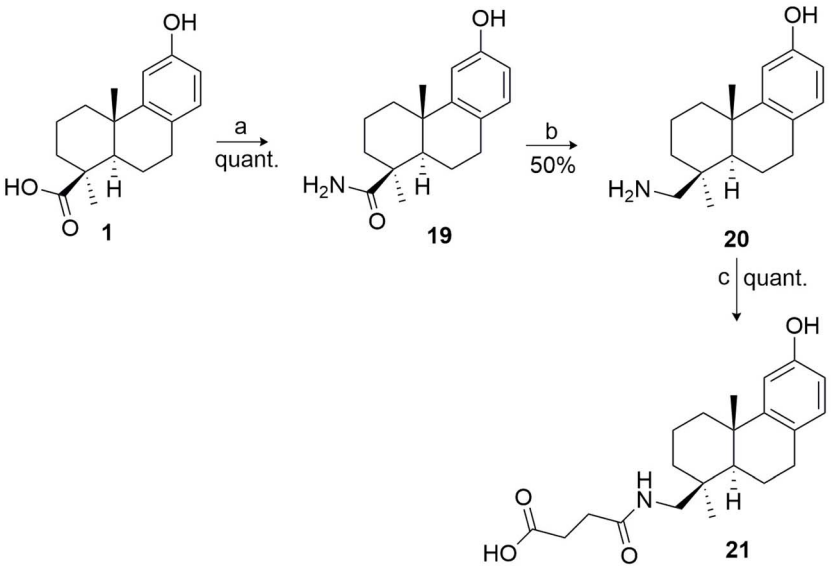

Scheme 4 Reagents and conditions. (a) DIPEA, HATU, NH_4Cl, dry DMF, r.t., 16 h; (b) $LiAlH_4$ 2M in THF, dry THF, 0 °C to r.t., 16 h; (c) succinic anhydride, DMAP, DCE, 0 °C to r.t., 30 min.

by deprotection with TFA and TFE in DCM, to provide the corresponding *N*-hydroxybutyl and penthyl amines **30** and **31** in 55% and 15% yields, respectively.

Analysis of the colistin adjuvant activity of the abietane diterpenoids

The colistin adjuvant activity of the compounds was analyzed by determining their effect on the growth of the *P. aeruginosa* colistin resistant strain PA14 Col^R5.[10] As colistin resistance in PA14 Col^R5 depends on the activity of the ArnT transferase, it is expected to be reduced by the compounds.[10] Of note, compounds targeting ArnT are not expected to possess antibacterial activity *per se*, as demonstrated by the comparable growth profile of *P. aeruginosa* parental strains and their isogenic Δ*arn* mutants.[10] To obtain measurable effects from the combination compound-colistin on the bacterial growth, the sublethal dose of 8 μg mL^{-1} of colistin, which reduces the PA14 Col^R5 growth to 50% (Fig. S1), was selected.[40] Based on this, pairwise interaction compound-colistin was analyzed by combining each compound, in a range of concentrations from 16 to 250 μM, with 8 μg mL^{-1} of colistin, the resulting effect was compared to the effect of the individual compounds. First, the *O*-derivatives (**2–8**) of compound **1**, which differed for the residue at C-16, were tested. These compounds showed a broad spectrum of adjuvant activity, from no effect to complete growth inhibition (Fig. 3A).

In particular, compounds **1**, **4**, and **8** did not reduce the growth of PA14 Col^R5, with compound **4** showing the opposite effect, namely, enhanced growth. Compounds **7** and **12** induced a marginal reduction in growth, while compounds **3**, **5**, and **6** caused a dose-dependent reduction in growth, ranging from 80 to 60%. Finally, compound **2** led to an almost complete inhibition of PA14 Col^R5 growth. The promising result obtained with **2** was further corroborated by repeating the assay with additional samples containing the compound-only. As expected, the growth reduction caused by compound **2** was greatest when combined with colistin and significantly less in the absence of colistin (Fig. 3B). This data supports the specificity of compound **2**, which differs from **1** for the presence of an alcohol group at C16, as its antimicrobial activity is approximately 20-fold higher when combined with colistin than in its absence. Differently, compounds **3**, **5**, and **6**, enhancing the distance between the acid function at C16 and the lipophilic portion of the abietane scaffold, maintained the capacity to reduce the growth of PA14 Col^R5, although at a reduced level compared to compound **2**. Otherwise, increasing the distance between the alcohol group at C16 and the lipophilic portion of the abietane scaffold appeared to completely abrogate the binding to ArnT, as demonstrated by the absence of colistin adjuvant activity of compound **12** (compare compounds **12** and **2** in Fig. 3A).

Finally, the possible effect of the C ring in mediating the interaction of the abietane scaffold with ArnT was studied by

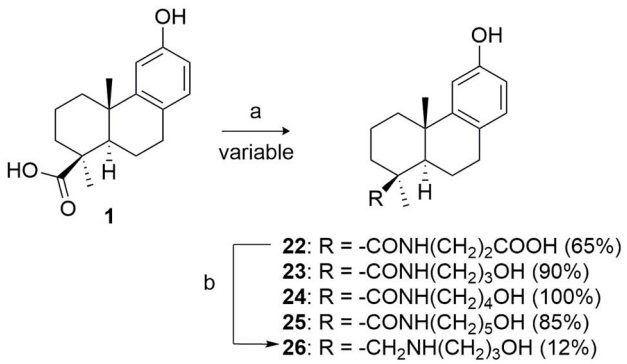

Scheme 5 Reagents and conditions. (a) DIPEA, HATU, $NH_2(CH_2)_nOH$ or $NH_2(CH_2)_2COOH$, dry DMF; (b) $LiAlH_4$ 2M in THF, dry THF, 0 °C to r.t., 32 h.

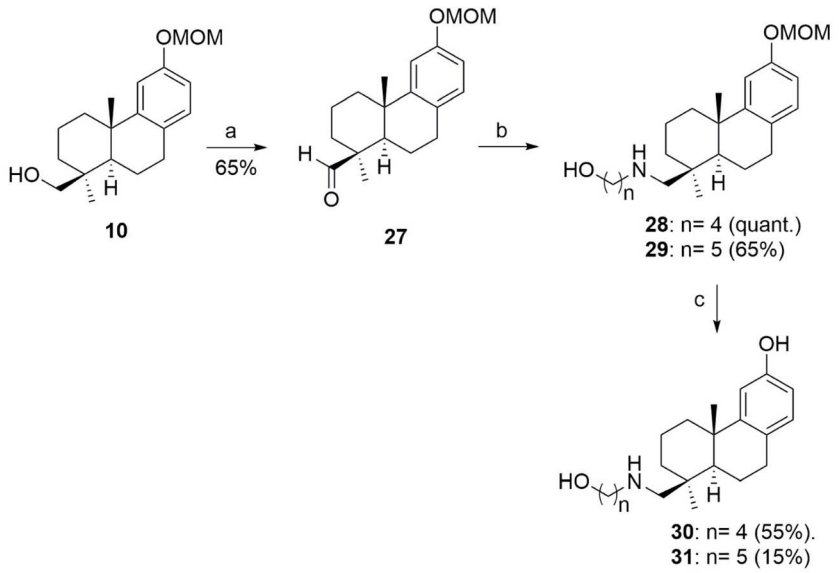

Scheme 6 Reagents and conditions. (a) DMP, $NaHCO_3$, dry CH_2Cl_2, 0 °C to r.t., 2 h; (b) $NH_2(CH_2)_nOH$, AcOH 1%, $NaCNBH_3$, dry CH_2Cl_2, r.t., 24 h; (c) TFA, TFE, CH_2Cl_2, 0 °C to r.t.

analyzing the antimicrobial activity of compounds **13–18** (Fig. 4).

Among these, compound **13** was the most active, with complete abrogation of PA14 Col^{R}5 growth at 250 μM. Compounds **14**, **15**, and **18** only partially reduced bacterial growth at the same concentration, from approximately 60% for **14** and **15** to 80% for **18**. Compound **18** maintained high activity even at 125 μM. While compounds **13**, **14**, and **18** appeared to be specific colistin adjuvants, as no growth inhibition was detected in the absence of colistin, compound **15** showed similar antibacterial activity irrespective of colistin (Fig. S2). Compounds **16** and **17** were shown to be the least active, exhibiting little to no growth inhibition (Fig. 4 and S3). Further, direct comparison of the activity of compounds **15–18** and **13** with that of the correlated ones **1**, **2**, **4**, **6** and **14**, respectively, showed that the methoxyl group at C-12 is associated with higher colistin adjuvant activity, except for compound **2**, in which the highest activity was associated with the hydroxyl group (Fig. S3).

The colistin adjuvant activity of the N-derivatives of compound **1** was determined using the same approach as reported above. Compounds **19**, **21**, and **22** showed only marginal growth inhibitory activity, while **20** inhibited the growth of PA14 Col^{R}5 by 70% (Fig. 5A). To assess the effect of enhancing the distance between the lipophilic portion and the polar function (alcohol group) of the abietane scaffold, amides **23–25** were tested (Fig. 5B).

Only compounds **24** and **25** showed some activity, with growth inhibition of approximately 60% and 80%, respectively, at the highest dose. Their specificity was demonstrated by negligible activity in the absence of colistin (Fig. S4). Similarly, the corresponding amines **30** and **31** exhibited a dose-dependent activity, while compound **26** showed no effect on PA14 Col^{R}5 growth (Fig. 5C). Additionally, the inhibitory activity on bacterial growth of compound **30** appeared significantly higher with colistin than in its absence at the concentration ranging from 63 to 250 μM (Fig. 6A).

Differently, the antimicrobial activity of compound **31** appeared to be independent of colistin, except at the highest concentration (Fig. 6B), possibly due to off-target effects. Finally, for a more direct comparison of the compounds showing colistin-dependent inhibition of *P. aeruginosa* growth, ranging from 50 to 99% at 250 μM, the growth inhibitory concentrations, IC_{50} and IC_{90}, were determined as reported in Materials and methods (Table 1). Based on the IC_{50}, the compounds that showed the highest activity (lowest IC_{50} values) were **18**, **13**, **30**, and **2**, all but **30** belonging to the oxygen derivative group. Among these, compound **18** also showed the lowest IC_{90}.

We confirmed the compound-colistin synergy for **18**, **13**, **30**, and **2** with chequerboard assays. As shown in Fig. 7, all compounds caused a dose-dependent reduction of PA14 Col^{R}5 growth. Compound **2** reduced the colistin MIC to 4 μg mL^{-1} at 250 μM, while compounds **13**, **18**, and **30** to 8 μg mL^{-1} at the same concentration.

Overall, this analysis confirmed that compounds **18**, **13**, **30**, and **2** act as bona fide nonantibiotic adjuvants of colistin as they potentiate colistin activity by targeting its *arn*-dependent resistant mechanism. Accordingly, these compounds, although showing no antimicrobial activity, reduce the MIC of colistin by 8- or 16-fold in the combined treatments. Finally, taking into consideration lung infection, the cytocompatibility of these compounds was evaluated in the bronchial epithelial cells 16HBE. For this, cells were treated with increasing concentration of the compounds and at two timepoints (3 and 18 h) cell viability was analyzed by the MTT assay. No significant changes in cell viability were observed under all conditions tested (Fig. 8).

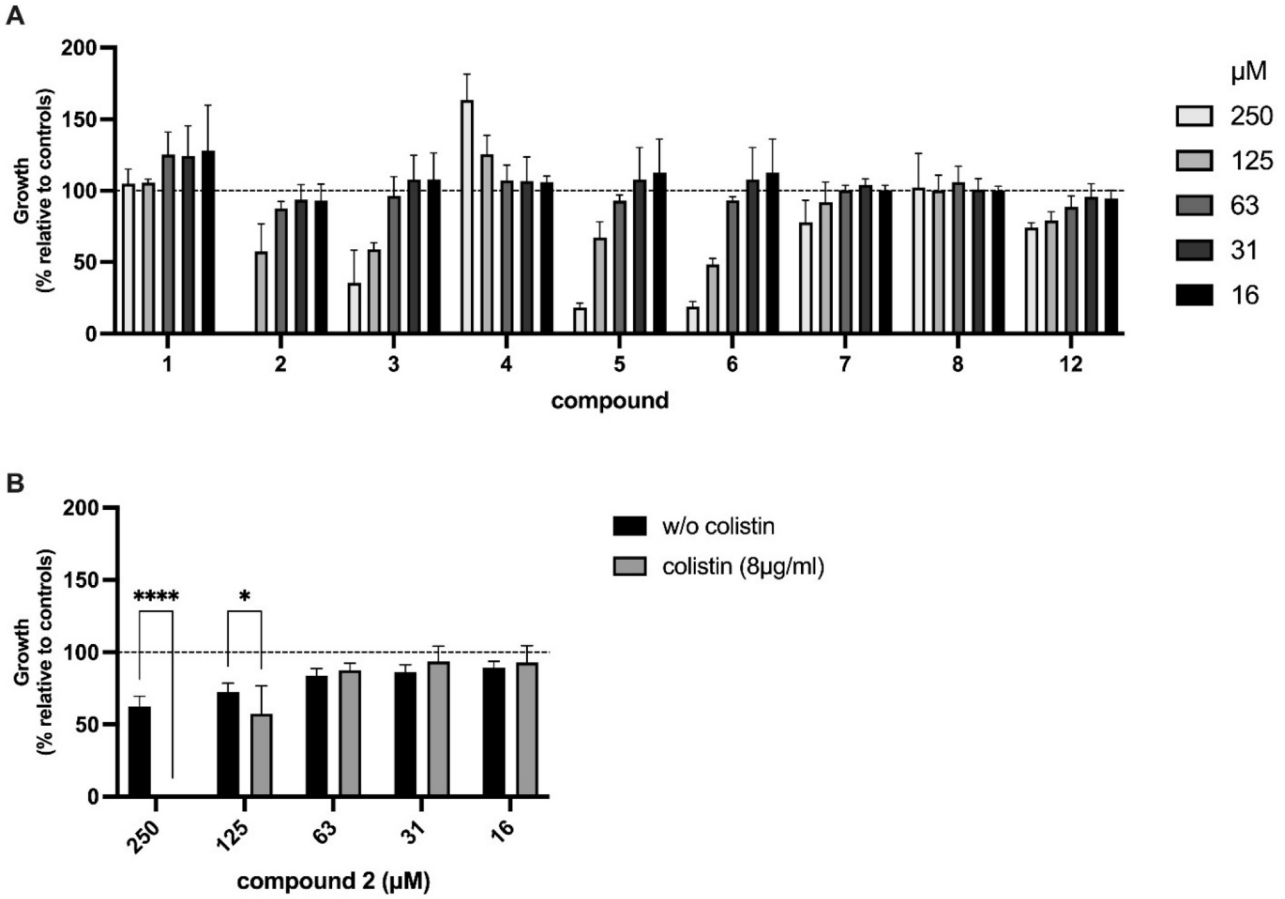

Fig. 3 Bacterial growth inhibition by compounds **1–8** and **12** (panel A) in the presence of sub-MIC concentration of colistin. (Panel B) Dose-dependent effect of compound **2** on bacterial growth in the presence of sub-MIC colistin (grey bar) or without colistin (black bar). Percent growth of PA14 Col^{R}5 was calculated on the growth with compound, at the indicated concentration, and colistin (8 μg mL^{-1}) relative to its respective control treated with equivalent concentrations of DMSO and colistin 8 μg mL^{-1} (100%, dotted line). Data are mean (±SD) of at least three independent experiments. *p < 0.05; ***p < 0,0001.

Binding studies on the most active ArnT inhibitors

The possible binding mode of the most active compounds **2**, **13**, **18**, and **30** to the ArnT protein from *P. aeruginosa* PA14 was investigated by molecular docking simulations. The previously developed protocol, which has been validated against the X-ray crystallography structure of *Cupriavidus metallidurans* ArnT, was adopted herein.[14,25,27] Given the lack of experimental structure of ArnT from *P. aeruginosa*, its three-dimensional structure was computationally built by AlphaFold2 using the Uniprot sequence coded by ID Q02R27.[41,42] Docking simulations were

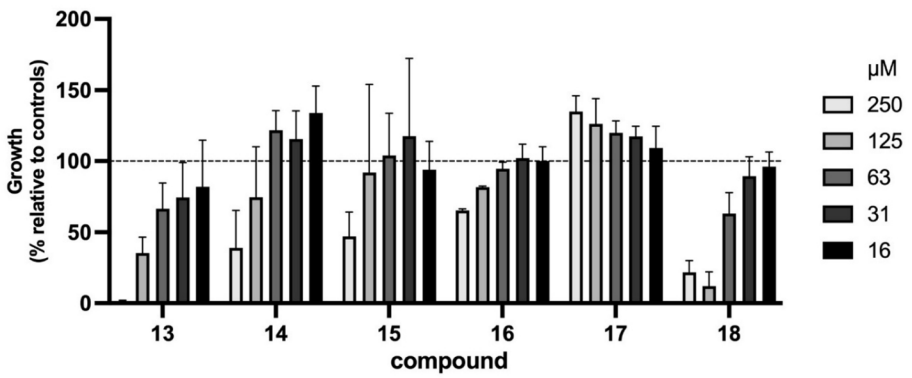

Fig. 4 Bacterial growth inhibition by compounds **13–18** in the presence of sub-MIC concentration of colistin. Percent growth of PA14 Col^{R}5 was calculated on the growth with compound, at the indicated concentration, and colistin (8 μg mL^{-1}) relative to its respective control treated with equivalent concentrations of DMSO and colistin 8 μg mL^{-1} (100%, dotted line). Data are mean (±SD) of at least three independent experiments.

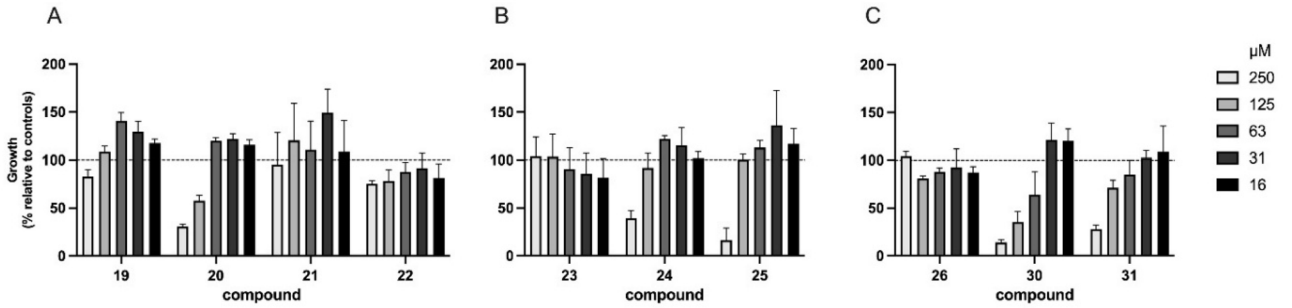

Fig. 5 Bacterial growth inhibition by compounds **19–22** (panel A), **23–25** (panel B) and **26–30** (panel C) in the presence of sub-MIC concentration of colistin. Percent growth of PA14 Col^{R}5 was calculated on the growth with compound, at the indicated concentration, and colistin (8 μg mL^{-1}) relative to its respective control treated with equivalent concentrations of DMSO and colistin 8 μg mL^{-1} (100%, dotted line). Data are mean (±SD) of at least three independent experiments.

carried out with the FRED docking program (OpenEye Cadence Molecular Sciences) (Fig. 9).[43]

While **2**, **18**, and **30** bind in a similar manner, **13** was found to bind with an opposite polarity, having the aromatic ring projected towards basic residues that bind the undecaprenylphosphate in the experimental ArnT structure.[14] In detail, **2** is H-bonded to the backbone of Ile29 through the phenolic OH group, while the aromatic ring is in a parallel displaced π–π stacking conformation to the side chain of Tyr131; the primary alcohol group is H-bonded to the side chain of Asp135 near the sugar binding pocket of the ArnT catalytic site. The aromatic ring of **13** is π–π stacked with the side chain of Tyr35, whereas the methoxyl moiety is H-bonded to Arg34; the methylester group at C4 is H-bonded to the side chain of Gln128. **18** binds similarly to **2**, although the functionalization inserted on the alkyl chain exploits additional interactions within the ArnT sugar binding pocket as well as with basic residues involved in the interaction with the undecaprenylphosphate substrate. Besides stacking to Tyr131, **18** establishes H-bonds with the side chain of Arg34 and Arg245. Finally, **30** shares binding hotspots with **2** and **18**, although the protonated amino group establishes a charge-assisted H-bond with the side chain of Asp135, and the primary alcohol group is H-bonded to Arg245 and Glu60. Docking scores, calculated with the Chemgauss4 function implemented in the FRED docking program, suggested

Table 1 Half maximum (IC_{50}) and 90% (IC_{90}) inhibitory concentration (μM) of the compounds against PA14 Col^{R}5

Compound	IC_{50}	IC_{90}	R^2*
18	73.91	182.49	0.87
13	80.79	267.01	0.82
30	96.36	217.10	0.80
2	130.50	225.94	0.89
6	130.70	276.74	0.86
5	156.20	311.44	0.85
20	166.70	341.57	0.77
31	171.90	432.90	0.80
25	225.10	259.22	0.70
24	227.00	365.42	0.74

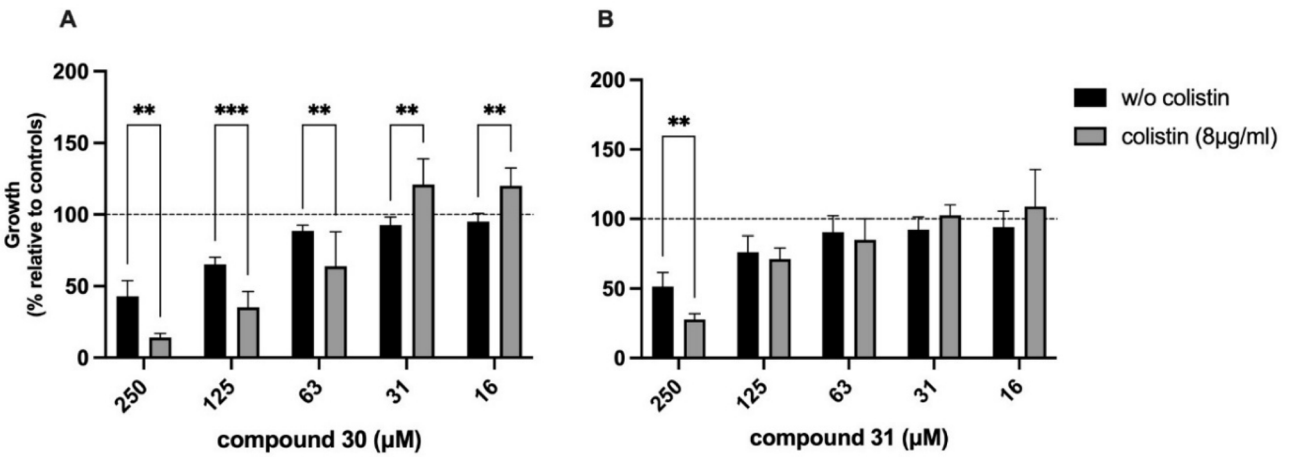

Fig. 6 Dose-dependent effect of compound **30** (panel A) and **31** (panel B) on PA14 Col^{R}5 growth after 24 h at 37 °C in MH supplemented with 8 μg mL^{-1} colistin (grey bar) or without colistin (black bar). Growth is expressed as percentage relative to control cultures treated with equivalent concentrations of DMSO. Data are mean (±SD) of at least three independent experiments. Statistics: two-way ANOVA with Bonferroni's multiple comparison test.

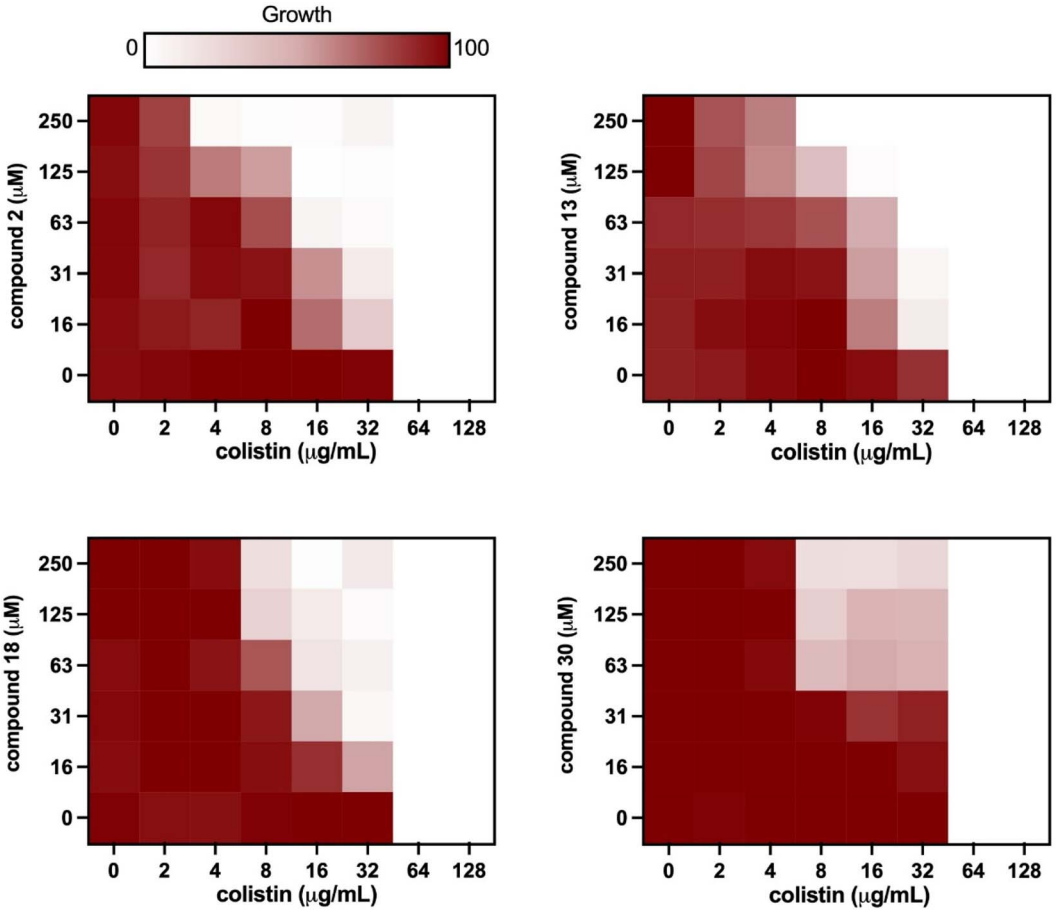

Fig. 7 Synergistic activity of compounds and colistin. Chequerboard assay between colistin and compound **2**, **13**, **18**, **30**. *Y* axis, compound (μM); *X* axis, colistin (μg mL^{-1}). Data are representative of two independent experiments for each pairwise analysis.

that the different binding polarity of **13** might account for a weaker binding affinity for the ArnT compared to **2**, **18** and **30** (Table 2).

Overall, docking results show that tested compounds are able to fit within the lipid A binding pocket of the ArnT catalytic site. The qualitative agreement between docking parameters and bioactivity data supports the proposed binding poses, allowing further rational optimization studies.

Notably, residues contacted by these molecules are highly conserved in the ArnT orthologs from multiple *P. aeruginosa* strains, as highlighted by sequence similarity analysis (Fig. S5).

In order to confirm that ArnT is the target of the compounds, a binding assay was performed. Because of the high fluorescence due to the aromatic ring of the PD derivatives, the **FDO** and the most active derivative **FDO-H** (compound 15 in Quaglio *et al.*, 2020),[27] which differs from the hit **FDO** by the absence of

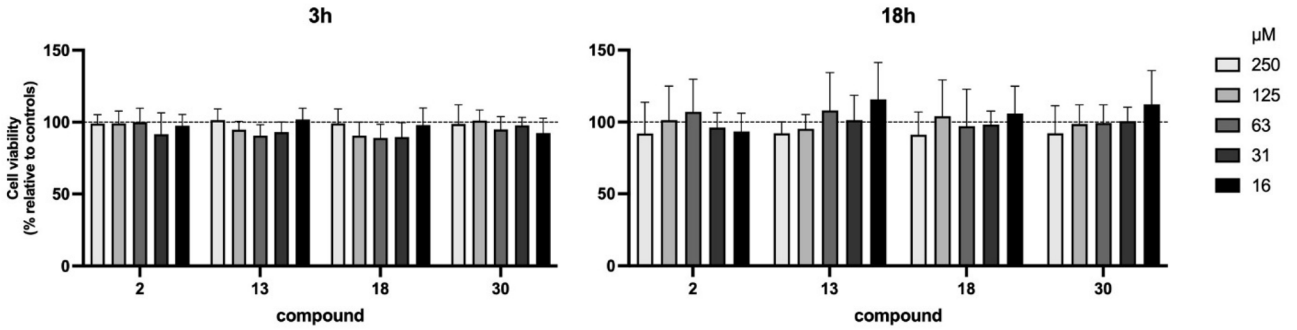

Fig. 8 Compound cytotoxicity. 16HBE cells viability were analyzed after exposure to the compounds at the indicated concentrations for 3 or 18 h. Cell viability, as assessed by the MTT assay, is expressed as a percentage relative to vehicle-only (DMSO) controls (dotted line). Data are the mean (±SD) of three independent experiments.

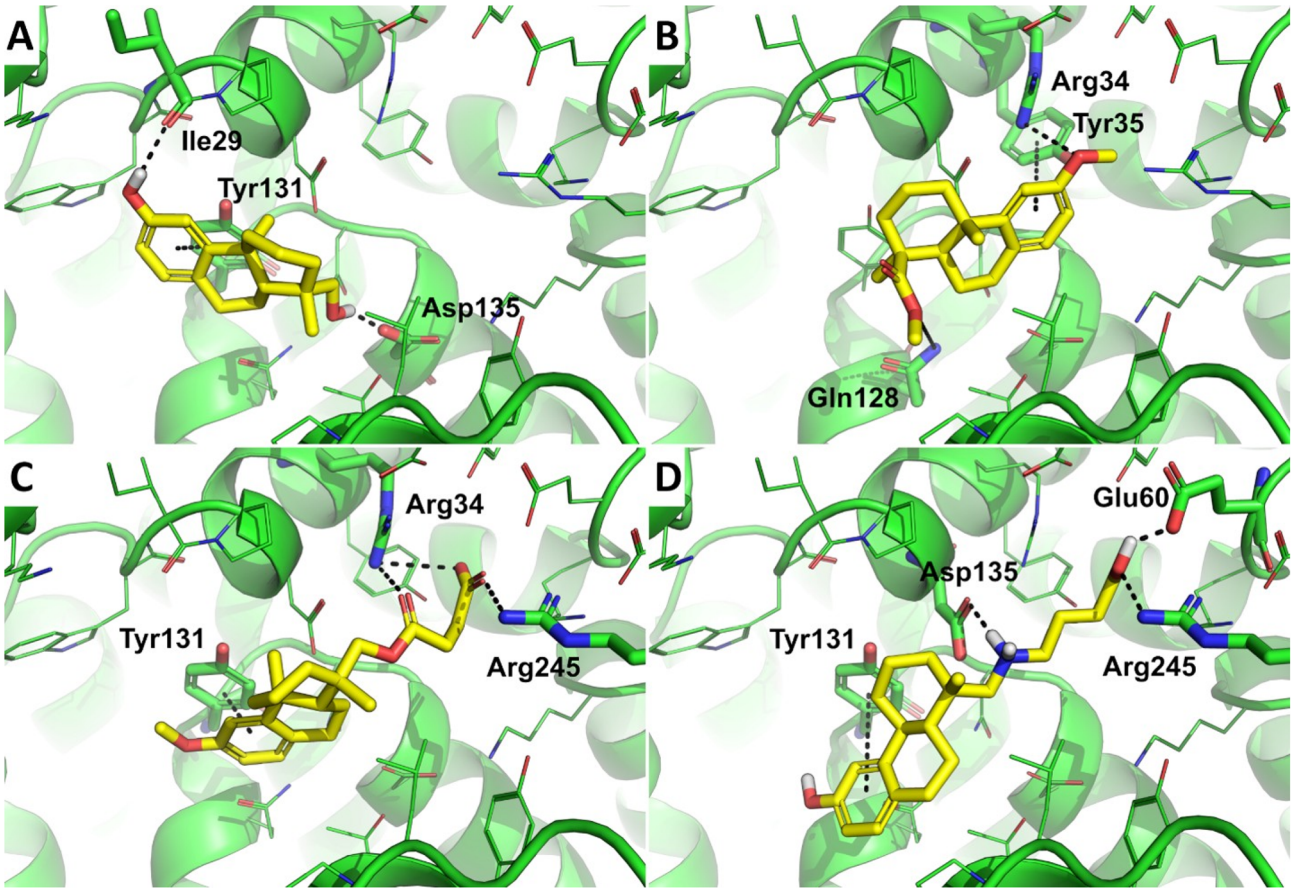

Fig. 9 Predicted binding mode of most active colistin adjuvants **2** (A), **13** (B), **18** (C), and **30** (D) towards the computational model of *P. aeruginosa* ArnT. Small molecules are shown as yellow sticks, ArnT is shown as green cartoon; residues within 5 Å from the ligands are shown as lines, while those contacted by each molecule are shown as sticks and are labeled. Residues numbering corresponds to the scheme of the UniProt ID Q02R27. Polar and stacking interactions are highlighted by black dashed lines.

the double bond between C-15 and C-16,[25,27] were employed to assess binding to recombinant *P. aeruginosa* ArnT by intrinsic tryptophan fluorescence spectroscopy. The lead compound **FDO** was initially assayed, but it showed high background, making analysis problematic; however, even in these conditions, a K_D of about 10 μM could be estimated. To obtain more reliable data, the **FDO-H** derivative was therefore employed. The choice of **FDO-H** is supported by previous molecular docking data, which show similar positioning of the PD compounds in the substrate binding site of ArnT.[27] Titration of ArnT with **FDO-H** caused quenching of tryptophan fluorescence (Fig. 10, upper panel). Analysis of the data yielded a K_D value close to 10 μM (Fig. 10, lower panel), substantiating the result obtained for **FDO**. This value is substantially lower than K_D 31.76 μM for isostevic acid,[28] in line with the higher potency of the lead compound **FDO-H**.

Structure–activity relationship

The naturally occurring aromatic abietane **1** and its newly synthesized twenty-four chemical derivatives highlighted that derivatives **2**, **13**, **18**, and **30**, belonging to the oxygen and nitrogen series, respectively, show the highest colistin adjuvant activity, causing an almost complete reduction of bacterial growth at 250 μM. At the same time, no effects were observed in the absence of colistin. Based on the overall outcomes of microbiological and computational investigations, a preliminary SAR was elaborated at two structural levels: the C-16 position at ring A and the C-12 position at ring C, and is graphically depicted in Fig. 11.

Concerning ring A, the reduction of the carbonyl group at C-16 and the presence of an alcohol group at the same position led to a high colistin adjuvant activity (**2**), causing an almost complete reduction of bacterial growth at 250 μM and 37% reduction at 125 μM, suggesting that an sp^3 hybridization favors the interaction of the compound with the catalytic site of ArnT.

An increased distance between the lipophilic portion of the terpene scaffold and the polar function, the alcohol group

Table 2 Chemgauss4 docking scores of **2**, **13**, **18**, **30**, and the two reference ArnT inhibitors

Compound	FRED Chemgauss4 score (dimensionless)
2	−6.18
13	−5.48
18	−6.87
30	−7.02

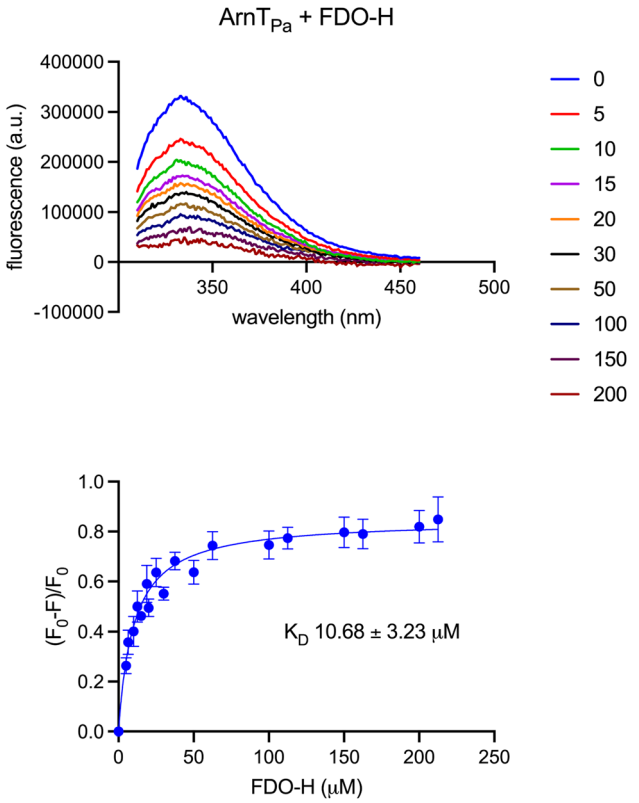

Fig. 10 Binding of FDO-H by *P. aeruginosa* ArnT: representative fluorescence spectra of recombinant *P. aeruginosa* ArnT titrated with FDO-H 5–200 μM (panel A); plot $(F_0 - F)/F_0$ of mean fluorescence at 333–337 nm *vs.* [FDO-H], $n = 8$ (panel B). The fit of the data to a one-site binding equation is shown.

linked at position C-16, maintains (**3**, **5**, **6**) the ability to reduce the growth of PA14 Col^{R}5. However, this effect is observed at a lower level compared to compound **2**. The introduction of an oxalyl group (**4**) completely abrogates the effect, probably due to the more rigid and planar conformation. Similarly, when a hindered group, such as a sugar moiety at C-16 (**7**, **8**), is present, the effect is completely nullified.

The substitution of oxygen with a nitrogen heteroatom in the functional group at C-16 of **1** shows a good colistin adjuvant activity at 250 μM, and only when the distance between the lipophilic portion of the scaffold and the polar function is enhanced (**24**, **25**). The reduction of the carbonyl group and the presence of a primary amine group at C-16 (**20**) partially inhibited the growth of PA14 Col^{R}5. The presence of a secondary amine featuring a 4-hydroxybutyl chain (**30**) resulted in a notable dose-dependent growth inhibition, which was significantly enhanced in the presence of colistin.

Concerning ring C, the methylation of the phenol group at the C-12 position led to a higher colistin adjuvant activity only in the presence of an acid or an ester group at the C-16 (**13**, **18**) position, compared to the phenol analogs (**14**, **6**). This trend, consistently observed across our experimental series, supports an empirical structure–activity relationship (SAR) suggesting that methylation at C-12 enhances the interaction of the aromatic scaffold with the biological target only when combined with specific polar functionalities at C-16. Although the mechanistic basis of this synergistic effect remains to be elucidated, it provides a valuable guideline for further optimization and mechanistic investigation.

Remarkably, microbiological assays coupled with molecular modeling indicated that for more efficient colistin adjuvant activity, likely resulting from the inhibition of ArnT activity by the selected compounds and therefore from their interaction with the catalytic site of ArnT, hydrogen bonding acceptor and donor groups at C-16 are required. The substitution of oxygen with a nitrogen heteroatom in the functional group at C-16 increases the biological activity in the amine series. Taken together, these findings outline a preliminary SAR profile centered on the abietane scaffold, highlighting the significance of specific hydrogen-bonding functionalities at C-16 and phenol

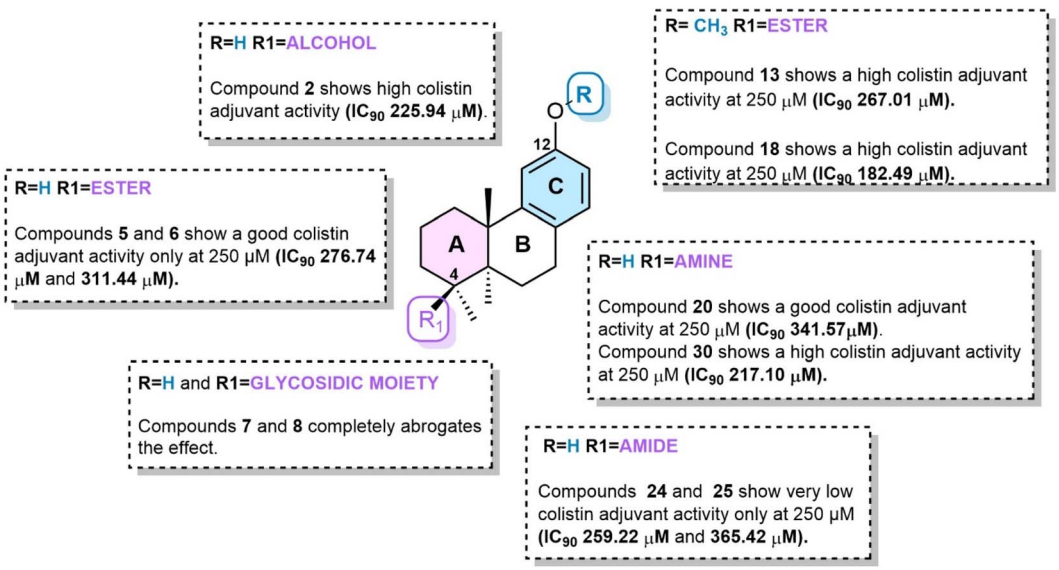

Fig. 11 SAR studies of podocarpic acid derivatives.

methylation at C-12 in modulating colistin adjuvant activity. These insights provide a rational framework for the further optimization of abietane-based ArnT inhibitors as next-generation colistin potentiators.

Conclusions

This study demonstrates the successful application of function-oriented synthesis to the design of abietane-based derivatives as colistin resistance breakers targeting the *P. aeruginosa* ArnT enzyme, with the final aim of systematic reduction and optimization of a complex natural scaffold toward pharmacologically relevant minimal structures. By leveraging the abietane scaffold of **1** as a rationally simplified mimic of *ent*-beyerene, we generated a library of analogues that retained or restored adjuvant activity against colistin-resistant *P. aeruginosa*. The most effective compounds, particularly **2**, **13**, **18**, and **30**, were able to restore colistin activity in resistant bacterial strains in a dose-dependent and colistin-dependent manner. Molecular docking supported the proposed binding mode of ArnT inhibitors and highlighted specific interactions at the catalytic site, notably involving the C-16 substituent and, in some cases, the methoxylated C-12 phenolic group. SAR analysis underscored the importance of hydrogen-bonding features, flexibility, and linker length between the lipophilic scaffold and polar functional groups. Moreover, nitrogen-based analogs such as compound **30** demonstrated effective colistin adjuvant activity, suggesting a viable strategy for further chemical development. Even if the relatively high IC_{50}/IC_{90} values of the most active compounds imply that these molecules require further optimization to improve their potency, these results establish the aromatic abietane scaffold as a valuable platform and FOS as a powerful design strategy for the development of next-generation colistin resistance breakers to overcome resistance in Gram-negative pathogens.

Author contributions

Silvia Cammarone and Valentina Pastore contributed equally to this work. CRediT: Silvia Cammarone and Valentina Pastore: validation, investigation, methodology, data curation, writing – original draft. Mariya Ryzhuk, Martina Cristoferi, Arianna Speroni and Davide Corinti: visualization, investigation, data curation. Francesco Imperi: visualization, writing – review & editing. Maria Carmala Bonaccorsi di Patti: validation, investigation, methodology. Bruno Botta: validation, writing – review & editing. Deborah Quaglio and Mattia Mori: conceptualization, methodology, investigation, supervision, funding acquisition, writing – original draft. Fiorentina Ascenzioni and Francesca Ghirga: conceptualization, methodology, investigation, resources, funding acquisition, writing – review & editing.

Conflicts of interest

There are no conflicts to declare.

Data availability

All data supporting the findings of this study are available within the article and its supplementary information (SI). Supplementary information is available. See DOI: https://doi.org/10.1039/d5ra09142j.

Acknowledgements

This research was supported by: EU funding within the MUR PNRR Extended partnership initiative on Emerging Infectious Diseases (Project no. PE00000007, INF-ACT) to MM; Progetto ECS 0000024 Rome Technopole, – CUP B83C22002820006, PNRR Missione 4 Componente 2 Investimento 1.5, finanziato dall'Unione europea – NextGenerationEU to SC, FG and DQ; PROGETTI MEDI ATENEO 2023 – RM123188F706283C to FG; Sapienza University (Medie Attrezzature Scientifiche_MA32218167926358) to FG; Sapienza, project 2023 – RG123188B49A8CB3 to FA. Mariya Ryzhuk was supported by the PNRR PhD scholarship funded by the Rome Technopole project. We thank OpenEye Cadence Molecular Sciences for their free academic license. This article is based upon work from COST Action EURESTOP, CA21145, supported by COST (European Cooperation in Science and Technology). We gratefully acknowledge Dr Giulia Mazzoccanti for her technical assistance with HPLC analyses.

References

1 B. Li and T. J. Webster, Bacteria antibiotic resistance: New challenges and opportunities for implant-associated orthopedic infections, *J. Orthop. Res.*, 2018, **36**, 22–32.
2 V. H. Krishnaprasad and S. Kumar, Antimicrobial Resistance: An Ultimate Challenge for 21st Century Scientists, Healthcare Professionals, and Policymakers to Save Future Generations, *J. Med. Chem.*, 2024, **67**, 15927–15930.
3 W. H. Organization, WHO publishes list of bacteria for which new antibiotics are urgently needed, https://www.who.int/en/news-room/detail/27-02-2017-who-publishes-list-of-bacteria-for-which-new-antibiotics-are-urgently-needed.
4 H. Wright, R. A. Bonomo and D. L. Paterson, New agents for the treatment of infections with Gram-negative bacteria: restoring the miracle or false dawn?, *Clin. Microbiol. Infect.*, 2017, **23**, 704–712.
5 H. Giamarellou, Epidemiology of infections caused by polymyxin-resistant pathogens, *Int. J. Antimicrob. Agents*, 2016, **48**, 614–621.
6 D. J. Payne, Desperately seeking new antibiotics, *Science*, 2008, **321**, 1644–1645.
7 L. Poirel, A. Jayol and P. Nordmann, Polymyxins: antibacterial activity, susceptibility testing, and resistance mechanisms encoded by plasmids or chromosomes, *Clin. Microbiol. Rev.*, 2017, **30**, 557–596.
8 F. A. Gogry, M. T. Siddiqui, I. Sultan and Q. M. R. Haq, Current update on intrinsic and acquired colistin

resistance mechanisms in bacteria, *Front. Med.*, 2021, **8**, 677720.

9 A. Sabnis, K. L. H. Hagart, A. Klöckner, M. Becce, L. E. Evans, R. C. D. Furniss, D. A. I. Mavridou, R. Murphy, M. M. Stevens and J. C. Davies, Colistin kills bacteria by targeting lipopolysaccharide in the cytoplasmic membrane, *eLife*, 2021, **10**, e65836.

10 A. Lo Sciuto and F. Imperi, Aminoarabinosylation of lipid A is critical for the development of colistin resistance in *Pseudomonas aeruginosa*, *Antimicrob. Agents Chemother.*, 2018, **62**, 10–1128.

11 E. M. Nowicki, J. P. O'Brien, J. S. Brodbelt and M. S. Trent, Extracellular zinc induces phosphoethanolamine addition to *Pseudomonas aeruginosa* lipid A *via* the ColRS two-component system, *Mol. Microbiol.*, 2015, **97**, 166–178.

12 T. Pedersen, J. O. Sekyere, U. Govinden, K. Moodley, A. Sivertsen, Ø. Samuelsen, S. Y. Essack and A. Sundsfjord, Spread of plasmid-encoded NDM-1 and GES-5 carbapenemases among extensively drug-resistant and pandrug-resistant clinical Enterobacteriaceae in Durban, South Africa, *Antimicrob. Agents Chemother.*, 2018, **62**, 10–1128.

13 M. Cervoni M, D. Sposato, A. Lo Sciuto and F. Imperi, Regulatory Landscape of the *Pseudomonas aeruginosa* Phosphoethanolamine Transferase Gene eptA in the Context of Colistin Resistance, *Antibiotics*, 2023, **12**, 200.

14 V. I. H. Petrou, C. M. Schultz, K. M. Clarke, O. B. Vendome, J. Tomasek, S. R. D. Banerjee, K. R. Belcher Dufrisne and M. Kloss, Structures of 51 aminoarabinose transferase ArnT suggest a molecular basis for lipid A glycosylation, *Science*, 2016, **351**, 608–612.

15 W. T. Barker, A. M. Nemeth, S. M. Brackett, A. K. Basak, C. E. Chandler, L. A. Jania, W. J. Zuercher, R. J. Melander, B. H. Koller and R. K. Ernst, Repurposing eukaryotic kinase inhibitors as colistin adjuvants in Gram-negative bacteria, *ACS Infect. Dis.*, 2019, **5**, 1764–1771.

16 A. M. Nemeth, A. K. Basak, A. W. Weig, S. A. Marrujo, W. T. Barker, L. A. Jania, T. A. Hendricks, A. E. Sullivan, P. M. O'Connor and R. J. Melander, Structure–Function Studies on IMD-0354 Identifies Highly Active Colistin Adjuvants, *ChemMedChem*, 2020, **15**, 210–218.

17 F. Cappiello, M. R. Loffredo, C. Del Plato, S. Cammarone, B. Casciaro, D. Quaglio, M. L. Mangoni, B. Botta and F. Ghirga, The revaluation of plant-derived terpenes to fight antibiotic-resistant infections, *Antibiotics*, 2020, **9**, 325.

18 B. Casciaro, L. Mangiardi, F. Cappiello, I. Romeo, M. R. Loffredo, A. Iazzetti, A. Calcaterra, A. Goggiamani, F. Ghirga and M. L. Mangoni, Naturally-occurring alkaloids of plant origin as potential antimicrobials against antibiotic-resistant infections, *Molecules*, 2020, **25**, 3619.

19 N. Jubair, M. Rajagopal, S. Chinnappan, N. B. Abdullah and A. Fatima, Review on the antibacterial mechanism of plant-derived compounds against multidrug-resistant bacteria (MDR), *Evidence-Based Complementary and Alternative Medicine*, 2021, **2021**, 3663315.

20 D. J. Newman and G. M. Cragg, Natural products as sources of new drugs over the nearly four decades from 01/1981 to 09/2019, *J. Nat. Prod.*, 2020, **83**, 770–803.

21 G. D. Wright, Opportunities for natural products in 21 st century antibiotic discovery, *Nat. Prod. Rep.*, 2017, **34**, 694–701.

22 S. E. Rossiter, M. H. Fletcher and W. M. Wuest, Natural products as platforms to overcome antibiotic resistance, *Chem. Rev.*, 2017, **117**, 12415–12474.

23 H. Lachance, S. Wetzel, K. Kumar and H. Waldmann, Charting, navigating, and populating natural product chemical space for drug discovery, *J. Med. Chem.*, 2012, **55**, 5989–6001.

24 S. Erazo, M. Zaldívar, C. Delporte, N. Backhouse, P. Tapia, E. Belmonte, F. Delle Monarche and R. Negrete, Antibacterial diterpenoids from Fabiana densa var. ramulosa, *Planta Med.*, 2002, **68**, 361–363.

25 F. Ghirga, R. Stefanelli, L. Cavinato, A. Lo Sciuto, S. Corradi, D. Quaglio, A. Calcaterra, B. Casciaro, M. R. Loffredo and F. Cappiello, A novel colistin adjuvant identified by virtual screening for ArnT inhibitors, *J. Antimicrob. Chemother.*, 2020, **75**, 2564–2572.

26 D. Quaglio, S. Corradi, S. Erazo, V. Vergine, S. Berardozzi, F. Sciubba, F. Cappiello, M. E. Crestoni, F. Ascenzioni and F. Imperi, Structural elucidation and antimicrobial characterization of novel diterpenoids from Fabiana densa var. ramulosa, *ACS Med. Chem. Lett.*, 2020, **11**, 760–765.

27 D. Quaglio, M. L. Mangoni, R. Stefanelli, S. Corradi, B. Casciaro, V. Vergine, F. Lucantoni, L. Cavinato, S. Cammarone and M. R. Loffredo, Ent-Beyerane diterpenes as a key platform for the development of ArnT-mediated colistin resistance inhibitors, *J. Org. Chem.*, 2020, **85**, 10891–10901.

28 V. Pastore, J. Frison, C. Pesce, M. Ryzhuk, M. Garofalo, M. Cristoferi, S. Cammarone, G. Fabrizio, M. C. B. Di Patti and D. Quaglio, Development of nanovehicles for co-delivery of colistin and ArnT inhibitors, *Int. J. Pharm.*, 2025, **675**, 125515.

29 M. A. González, Synthetic derivatives of aromatic abietane diterpenoids and their biological activities, *Eur. J. Med. Chem.*, 2014, **87**, 834–842.

30 M. A. González, Aromatic abietane diterpenoids: Their biological activity and synthesis, *Nat. Prod. Rep.*, 2015, **32**, 684–704.

31 S. Ichikawa, Function-Oriented Synthesis: How to Design Simplified Analogues of Antibacterial Nucleoside Natural Products?, *Chem. Rec.*, 2016, **16**, 1106–1115.

32 P. A. Wender, V. A. Verma, T. J. Paxton and T. H. Pillow, Function-oriented synthesis, step economy, and drug design, *Acc. Chem. Res.*, 2008, **41**, 40–49.

33 I. Y. Strobykina, O. V. Andreeva, B. F. Garifullin, R. R. Sharipova and V. E. Kataev, First conjugate of glucuronic acid with triterpenoid dihydrobetulin, *Russ. J. Gen. Chem.*, 2017, **87**, 579–582.

34 A. V. Demchenko, *Handbook of Chemical Glycosylation: Advances in Stereoselectivity and Therapeutic Relevance*, John Wiley & Sons, 2008.

35 I. Y. Strobykina, B. F. Garifullin, R. R. Sharipova, A. D. Voloshina, A. S. Strobykina, A. B. Dobrynin and V. E. Kataev, Synthesis and antimicrobial activity of

dihydrobetulin N-acetylglucosaminides, *Chem. Nat. Compd.*, 2017, **53**, 1101–1106.

36 K. A. Muñoz and P. J. Hergenrother, Facilitating compound entry as a means to discover antibiotics for gram-negative bacteria, *Acc. Chem. Res.*, 2021, **54**, 1322–1333.

37 S. Hummelgaard, J. P. Vilstrup, C. Gustafsen, S. Glerup and K. Weyer, Targeting PCSK9 to tackle cardiovascular disease, *Pharmacol. Ther.*, 2023, **249**, 108480.

38 D. B. M. Dess and J. C. Martin, Readily accessible 12-I-5 oxidant for the conversion of primary and secondary alcohols to aldehydes and ketones, *J. Org. Chem.*, 1983, **48**, 4155–4156.

39 O. I. K. Afanasyev, E. Kuchuk, D. L. Usanov and D. Chusov, Reductive amination in the synthesis of pharmaceuticals, *Chem. Rev.*, 2019, **119**, 11857–11911.

40 P. Yeh, A. I. Tschumi and R. Kishony, Functional classification of drugs by properties of their pairwise interactions, *Nat. Genet.*, 2006, **38**, 489–494.

41 UniProt Consortium, Uniprot: the universal protein knowledgebase in 2025, *Nucleic Acids Res.*, 2025, **53**, D609–D617.

42 J. Jumper, R. Evans, A. Pritzel, T. Green, M. Figurnov, O. Ronneberger, K. Tunyasuvunakool, R. Bates, A. Žídek and A. Potapenko, Highly accurate protein structure prediction with AlphaFold, *Nature*, 2021, **596**, 583–589.

43 M. McGann, FRED pose prediction and virtual screening accuracy, *J. Chem. Inf. Model.*, 2011, **51**, 578–596.